Nucleosome mobilization by ISW2 requires the concerted action of the ATPase and SLIDE domains

Published in final edited form as:
Nat Struct Mol Biol. 2013 February ; 20(2): 222–229. doi:10.1038/nsmb.2486.

Nucleosome mobilization by ISW2 requires the concerted action of the ATPase and SLIDE domains

Swetansu K. Hota[1,‡], **Saurabh K. Bhardwaj**[1,‡], **Sebastian Deindl**[2,3], **Yuan-chi Lin**[1], **Xiaowei Zhuang**[2,3,4], and **Blaine Bartholomew**[1,*]

[1]Department of Biochemistry and Molecular Biology, Southern Illinois University School of Medicine, Carbondale, IL. 62901-4413 U.S.A

[2]Howard Hughes Medical Institute, Harvard University, Cambridge, Massachusetts 02138, USA

[3]Department of Chemistry and Chemical Biology, Harvard University, Cambridge, Massachusetts 02138, USA

[4]Department of Physics, Harvard University, Cambridge, Massachusetts 02138, USA

Abstract

The ISWI family of ATP-dependent chromatin remodelers represses transcription by changing nucleosome positioning. The interactions with extranucleosomal DNA and the requirement of a minimal length of extranucleosomal DNA by ISWI mediate the spacing of nucleosomes. ISW2 from *Saccharomyces cerevisiae,* a member of the ISWI family, has a conserved domain called SLIDE (SANT-like ISWI domain), whose binding to extranucleosomal DNA ~19 bp from the edge of nucleosomes is required for efficiently pushing DNA into nucleosomes and maintaining the unidirectional movement of nucleosomes, as reported here. Loss of SLIDE binding does not perturb ATPase domain binding to the SHL2 site of nucleosomes or its initial movement of DNA inside of nucleosomes. ISW2 has therefore two distinct roles in mobilizing nucleosomes, with the ATPase domain translocating and moving DNA inside nucleosomes, and the SLIDE domain facilitating the entry of linker DNA into nucleosomes.

Nucleosome movement by ATP-dependent chromatin remodelers contribute to the dynamic nature of chromatin[1–4]. All of these chromatin remodelers have a DNA-dependent ATPase domain belonging to the SF2 family of helicases that provides the mechanical force to mobilize nucleosomes. One class of these remodelers is the ISWI family which is responsible for changing nucleosome positions at the 5′ and 3′ ends of genes. In *Saccharomyces cerevisiae* there are three ISWI complexes called ISW1a, ISW1b and ISW2. Isw2 refers to only the catalytic subunit and ISW2 to the complex containing four subunits (Itc1, Dpb4, Dls1, and Isw2). ISWI remodelers require a minimal length of extranucleosomal DNA for mobilizing nucleosomes[5–9] and three of the four subunits of ISW2 bind to extranucleosomal DNA[7, 10, 11, 14, 15]. Although the auxiliary subunits of ISW2 greatly contribute to the activity of the complex, the catalytic subunit alone can also

*Corresponding author. Mailing address: Department of Biochemistry and Molecular, Biology, Southern Illinois University School of Medicine, 1245 Lincoln Dr., Neckers, Bldg. Room 229, Carbondale, IL 62901-4413., Phone: (618) 453-6437. Fax: (618) 453-6440. bbartholomew@siumed.edu.
‡equally contributed to this paper

AUTHORS CONTRIBUTION

S.K.H., S.K.B., S.D., X.Z. and B.B. experimental design. S.K.H., S.K.B. S.D. and Y.L. performed experiments. S.K.H., S.D., X.Z. and B.B. wrote the paper.

COMPETING FINANCIAL INTERESTS

The authors declare no competing financial interests.

mobilize nucleosomes. The C-terminus of Isw2 is required for its remodeling activity and the SLIDE domain in the C-terminus binds extranucleosomal DNA[12]. The SLIDE (SANT-like ISWI domain) domain was first discovered in Drosophila after solving the crystal structure of the C-terminus of ISWI and has a structure similar to the SANT (Swi3, Ada2, NCoR, TFIIIB) domain found in a variety of transcription factors and chromatin modifiers[13, 14]. The SLIDE domain from ACF in Drosophila and from ISW1a in *Saccharomyce cerevisiae* have been shown to bind DNA[14, 15]. We have investigated the role of the SLIDE domain and its binding to extranucleosomal DNA in ISW2 remodeling and demonstrate it contributes to moving DNA into nucleosomes.

Result

ISW2 assembly and remodeling requires the SLIDE domain

We found the SLIDE domain to be required for ISW2 complex integrity (Fig. 1). Deletion of the SLIDE domain disrupted the ISW2 complex and eliminated Itc1 binding to Isw2 (Fig. 1a and 1b, lane 1 and 2, and data not shown). The SLIDE domain in ISW1a and ISW1b has a similar role in complex assembly[16]. The SANT domain is also required for complex assembly in ISW1b, but not in any other ISWI remodeler investigated so far. Drosophila ISWI required a region next to the SLIDE domain called the ACF1 interaction domain (AID) and not the SANT and/or SLIDE domains[17] for binding ACF1 to ISWI. An AID-like domain does not exist in Isw2 since the extreme C-terminus of Isw2 was not required for complex integrity (Fig.1b lane 3). Full length Isw2 bound DNA and nucleosomes with 1/2.5 and 1/5 the affinity of the complete ISW2 complex (Supplementary Fig. 1a and 2a, compare lanes 2–7 to lanes 14–19,and Supplementary Fig. 1b and 2b, compare ISW2 to Isw2). The auxiliary subunit Itc1 and its binding to extranucleosomal DNA markedly increase the affinity of the complex for nucleosomes. Isw2 without the SLIDE domain bound free DNA and nucleosomes as well as full length Isw2 (Supplementary Fig. 1a and 2a, compare lanes 8–13 to lanes 14–19 and Supplementary Fig. 1b and 2b, compare ΔSLIDE to Isw2) and when bound to nucleosomes was resistant to competition with excess free DNA unlike full length Isw2 (Supplementary Fig. 2c, compare lanes 6–9 to lanes 10–13). Isw2 subunit lacking the SLIDE domain moved nucleosomes ~20 times less efficiently than the Isw2 subunit alone even though both have comparable affinity for nucleosomes (Supplementary Fig. 3a, compare lanes 2–6 to 12–16 and Supplementary Fig. 3b, compare Isw2 to ΔSLIDE). The two roles of the SLIDE domain are to increase the affinity for nucleosomes by binding to Itc1 and to facilitate the nucleosome mobilizing activity of the catalytic subunit.

Mutations in the SLIDE domain reduce binding to linker DNA

Four basic amino acid residues in SLIDE were predicted to be involved in binding DNA based on a structural model constructed from the X-ray crystal structures of the C-terminus of Drosophila ISWI (PDB accession number 1OFC) and Isw1 (PDB accession number 2Y9Z) from *Saccharomyces cerevisiae* (Fig. 1c and 1d). The DNA binding helix of the SLIDE domain in Drosophila ISWI is nearly twice the length of the same helix in Isw1a (Supplementary Fig. 4) and presumably is more similar to that in Isw2. Only a subset of the conserved positively charged residues in the SLIDE domain of Isw2 probably bind DNA based on crosslinking data and structural modeling (Fig. 1e). Alignment of the model of the Isw2 SLIDE domain with the structure of the Isw1a SLIDE domain bound to DNA suggests the conserved basic residues Arg992, Lys1046, Arg1047, and Arg1057 in Isw2 to bind to extranucleosomal DNA (Fig. 1c and 1d). These residues are in the region of SLIDE shown to crosslink to linker DNA 19 bp from the entry site of nucleosomes[15]. Residues Lys1046, Arg1047 and Arg1057 are predicted to be in the 3rd α helix of SLIDE and Arg992 in an adjacent loop. Removal of these positively charged residues by alanine substitution did not

disrupt ISW2 complex integrity (Fig.1b lane 5) and the mutant complex is referred to as mSLIDE.

Most of the interactions of ISW2 with nucleosomes were not changed in mSLIDE as observed by protection of DNA from cleavage with hydroxyl radicals. Under full binding conditions wild type (WT) and mSLIDE bound to extranucleosomal DNA (nt −70 to −110), the edge of nucleosomes (nt −49 and −59), and Superhelical Location (SHL) 2 at nt −19 as shown by DNA protection (Fig. 2a and 2b). Mutations in SLIDE weakened ISW2 binding to the same stretch of extranucleosomal DNA previously shown to be proximal to the SLIDE domain by DNA crosslinking as shown by protection from nt −80 to −94 being reduced or lost with mSLIDE (Fig 2b & 2c). Reduction in SLIDE binding did not affect the other interactions of ISW2 such as the ATPase domain at SHL2. Lifting off of the ATPase domain that occurs when extranucleosomal DNA length is shortened does not seem to be caused by loss of SLIDE domain binding[9].

The interactions of mSLIDE with nucleosomes were examined further by photocrosslinking proteins to the phosphate backbone of DNA through a short ~7Å tether at 3 bp increments along extranucleosomal DNA and half helical turn increments in nucleosomal DNA (Fig. 3a–b)[18]. Isw2 crosslinking at nt −84, −90, −93, −96 and −111 decreased when mSLIDE was bound compared to WT consistent with changes in DNA protection (Fig. 3c). Isw2 crosslinking at nt −33 in the DNA gyre away from histone octamer was the same with mSLIDE and WT and showed that Isw2 binding to SHL2 had not been affected (Fig. 3d). The loss of Isw2 crosslinking in mSLIDE at nt −47 did not coincide with DNA footprinting due to it facing in toward the histone octamer and remaining protected even in the absence of Isw2 (Fig 3e). There are other changes in DNA crosslinking that don't correlate with changes in DNA protection and are likely due to the 7 Å reach of the crosslinker and to conformational changes rather than loss of binding to DNA. The auxiliary subunit Itc1 crosslinked more at nt −84 in extranucleosomal DNA and inside of nucleosomes at nt −22 with mSLIDE than WT (Fig. 3f–h). Site-directed DNA crosslinking showed mutations in SLIDE reduced binding of Isw2 to extranucleosomal DNA in a region spanning from nt −84 to −93 without disrupting those near SHL2. While much of the ISW2 interactions with nucleosomes are maintained in mSLIDE, DNA crosslinking also suggests there are a few other changes besides reduced binding of SLIDE to extranucleosomal DNA that could have occurred.

The observed K_D of WT and mSLIDE were 20.0±1.5 and 34.8±1.4 nM using a fixed amount of nucleosomes and titrating with enzyme (Supplementary Fig. 5). The slight reduction in mSLIDE affinity for nucleosomes is consistent with mutations in SLIDE not affecting the binding of other parts of ISW2 to nucleosomes. The affinities of mSLIDE and WT for 50 bp of DNA were also not markedly different (27.9 nM ±0.95 versus 28.0 nM ±0.27, respectively). The electrophoretic mobilities of mSLIDE-DNA and mSLIDE-nucleosome complexes were generally slower than their WT counterparts (Supplementary Fig. 5a, compare lanes 8–9 to 16–17 and Supplementary Fig. 5c, compare lanes 2–9 to 10–17). This difference in mobility does not seem to be due to more than one ISW2 being bound per DNA or nucleosomes. Free ISW2 and mSLIDE are both monomeric complexes with apparent molecular weights of ~200–300 KDa as shown by glycerol gradient analysis (Supplementary Fig. 6a). The majority of mSLIDE bound to 50 bp of DNA behaves as a monomer like WT, but a minor fraction of complexes sedimented faster consistent with a small fraction of mSLIDE binding to DNA as a dimer (Supplementary Fig. 6b). The altered mobility of mSLIDE-DNA complexes reflects mostly a conformational change rather than dimerization of ISW2.

SLIDE domain binding to linker DNA required for remodeling

The binding of the SLIDE domain to extranucleosomal DNA can regulate the nucleosome mobilization activity of ISW2 without disrupting binding of the ATPase domain to nucleosomes. Nucleosomes were remodeled 4 times less efficiently with mSLIDE than WT when titrating enzyme versus nucleosomes (Fig. 4). Rates of nucleosome movement measured under fully bound conditions assessed the catalytic differences between WT and mSLIDE, and eliminated differences due to binding affinities. The rate of nucleosome movement was 9 times slower with mSLIDE than WT (0.066 ± 0.015 versus 0.62 ± 0.06 nM nucleosomes remodeled per sec, Fig 4b and 4d). The reduction in remodeling was primarily not caused by uncoupling of ATP hydrolysis from nucleosome movement since the rate of ATP hydrolysis was 7 times lower with mSLIDE under these same conditions (5.7±2.5 versus 40±8.0 fmoles Pi released per sec, Fig. 4e). Reduced binding of the SLIDE domain to extranucleosomal DNA interfered with nucleosome movement even though most ISW2 interactions were maintained as shown earlier by DNA protection and site-directed crosslinking. SLIDE domain binding to extranucleosomal DNA seems to have an important role in remodeling distinct from tethering the ATPase domain to nucleosomes.

We examined the interplay between the SLIDE and ATPase domains by reducing the ATPase domain binding to the SHL2 position through removal of the histone H4 N-terminal tail[9, 12]. If mutations in SLIDE were primarily affecting remodeling by negative regulation of the ATPase domain, then combining SLIDE mutations with H4 tail deletions will likely not have much of an additive effect. WT moved nucleosomes slower in the absence of the H4 tail and after 15 min reached steady state conditions (Fig. 4c lanes 2–8). The mSLIDE complex however was unable to move nucleosomes to any detectable extent after even 2 hr when the H4 tail was absent (Fig 4c lanes 9–16). We suggest that each domain likely performs distinct operations that are required for mobilizing nucleosomes and only the combination of weakened binding of the SLIDE and ATPase domains eliminated remodeling.

SLIDE binding facilitates DNA movement into nucleosomes

We measured the dynamic changes in histone-DNA contacts during remodeling at several reference points inside of nucleosomes to find how reduced binding of the SLIDE domain impacts nucleosome movement. Because of the time resolution we observed kinetic steps that are likely composed of multiple shorter remodeling steps that were not resolved. The reference points were at five positions inside of nucleosomes; at the dyad axis, and 37, 39 and 54 bp from the dyad axis (Fig 5 and Supplementary Fig. 7). We examined each position by coupling a photoreactive group to a site in the histone octamer proximal to DNA, photocrosslinking at different times during remodeling, and the DNA sites crosslinked to the particular parts of the histone octamer determined by cleavage[19, 20] (Fig. 5a). The nucleotide position of the cleavage site refers to the number of nt from the starting dyad position and are either + or − depending on whether they are respectively on the entry or exit sides of nucleosomes (Fig 5b).

We found nucleosome movement to be comprised of temporally distinct steps with DNA movement occurring faster on the exit side of the ATPase domain than on the entry side. Two of the sites probed are close to the bound ATPase domain with one on the entry side at nt +37 and the other on the exit side at nt +4/−4 about equal distance from the ATPase domain. While the changes at nt +4/−4 reached steady state conditions by 20 s and were completely shifted from their original position (Fig. 5c), those at nt_+37 were only nearly complete after 80 s (Fig. 5d). DNA moved 44 bp from near the dyad axis with cleavage changing from +4 to +48 after 20 s, but at nt +37 had only moved 34 nt with a new cleavage site at +71. We observed movement on the entry side to be slower when probed farther from

the ATPase domain and closer to the edge of the nucleosome at nt +54, comparable to that at nt +37 (Supplementary Fig. 7b). The progression in DNA movement from the dyad axis to the exit side of nucleosomes lagged in comparison to the rate of movement initially occurring at the dyad axis. Most of the original DNA position did not shift at nt −39 and nt −54 until after 80 s of remodeling (Fig. 5e and Supplementary Fig. 7c) and more closely resembled the rate of change on the entry side of the ATPase domain. After 80 s of remodeling, we found that DNA movement at all 5 reference points appeared to have caught up with each other with a total distance of 45–51 nt and a minor population as far as 58 (from nt +54) and 61 nt (from nt −39).

We observed DNA movement at the dyad axis being slower and the distance moved reduced with loss of SLIDE binding, however most nucleosomes moved after 80 s with mSLIDE (Fig. 5f). DNA moved only 10 nt with mSLIDE as seen by the cleavage site shifting from nt +4 to +14 and was considerably shorter than the 44 nt step with WT under comparable conditions (Fig. 5i, j). The fraction of nucleosomes with DNA shifting positions was less when probed between the dyad axis and the exit side 7–18 nt from starting positions at nt −39 and nt −54 similar to that at the dyad axis, there was an appreciably smaller fraction of nucleosomes that moved (Fig. 5h, j and Supplementary Fig. 7e,g). The mSLIDE appeared to first move DNA a step of 10 nt near the dyad axis before stalling and without further movement at the dyad axis to be less prone to propagate DNA movement through to the exit end of nucleosomes. The reason for the ATPase domain not being able to continue moving DNA through the nucleosome is tied to the lack of SLIDE interactions at the entry side and to the lack of DNA movement on the entry side of nucleosomes. DNA movement on the entry side was more adversely affected by the loss of SLIDE binding than was movement at the dyad axis or the exit side of nucleosomes. The mSLIDE complex after 20 and 80 s of remodeling did not markedly move DNA on the entry side of nucleosomes at nt +37 or +54 (Fig. 5g, j and Supplementary Fig. 7d, g), but WT moved DNA 18–58 bp from these same starting positions (Fig. 5 d,i and Supplementary Fig. 7b, f,). Stable binding of SLIDE domain to extranucleosomal DNA appears to be required to push DNA into nucleosomes at the entry site and without this the ATPase domain can only make one step of 10 nt. Further movement of the ATPase domain probably becomes too restricted due to lack of additional DNA coming into nucleosomes. These mutations in SLIDE while substantially slowing down the pushing of DNA into nucleosomes do not completely block nucleosomes remodeling, because with sufficient time mSLIDE can move nucleosomes to the appropriate final position (Fig. 4a).

DNA protection assays of mSLIDE-nucleosome complexes were done at short time intervals in the presence of ATP to examine how mSLIDE might move nucleosomal DNA (Fig. 6). First, we found that the additional interactions of ISW2 with nucleosomal DNA formed upon ATP hydrolysis and associated with template commitment required stable binding of the SLIDE domain to extranucleosomal DNA. There were no obvious changes in DNA protection in the mSLIDE-nucleosome complex from the entry side to the dyad axis after addition of ATP at the times sampled (Fig. 6d–g). WT has shown to go through first an early stage of ISW2 protection expanding from SHL-6 to SHL-1 in the first 5 s, followed by DNA in this same region becoming more accessible from apparently lifting off from the histone octamer[10]. The lifting off of DNA from the histone octamer is apparent by cleavage increasing in the trough regions without the amount of cleavage changing in the peak regions (Fig. 6b compared to 6a). We observed lifting off of nucleosomal DNA in the first DNA gyre coupled with additional protection in the second gyre from SHL+1 to +3 (Fig. 6b–c).

The protection assays also distinguished if the changes in histone-DNA contacts observed in Fig. 5 near the dyad axis and towards the exit side were due to changes in DNA

conformation such as helical pitch or formation of bulges, or were due to alterations in the histone octamer structure. Changes in DNA protection occurred in the side where DNA exits during remodeling (Fig 6e–g) and coincides well with changes in the mapped histone-DNA contacts (Fig. 5 and Supplementary Fig. 7). There was an increase in cutting associated with remodeling that started at the SHL+1→+2 region (15 s) which with more time expanded to SHL0→SHL+2 (30 s) and SHL0→SHL+3 (80 s). Cleavage increased in the troughs where DNA was protected by the histone octamer which could be caused by transiently lifting DNA off from the histone octamer. The enhanced cutting at the peak regions could be from the adjacent ATPase domain twisting and causing DNA structural changes that might make DNA more reactive to hydroxyl radicals. Alterations were not initially observed immediately adjacent to the ATPase domain binding region as might be expected. Distortions in DNA and its path on the histone octamer are probably transferred rapidly and stalled at the closest region(s) that are more pliable and energetically favorable. The SHL2 site is ideal in these terms since it is more prone to accommodate overtwisting of DNA[21–23] and to have less of a barrier for pulling DNA from than other positions[24, 25]. We found DNA bending does not account for the 10 bp shift in histone-DNA contacts found at the dyad axis with mSLIDE since there are no changes in the DNA protection pattern at this location. Mostly likely changes in histone-DNA contacts at the dyad axis are due to alterations in the histone octamer structure rather than in DNA. The ATPase domain as it translocates and rotates a short distance on DNA could push up against the histone octamer and thereby alter its structure.

SLIDE domain required for unidirectional DNA movement

Next, we examined DNA exiting nucleosomes during remodeling by single molecule Fluorescence Resonance Energy Transfer (smFRET). Nucleosomes were labeled with Cy3 on cysteine 120 of histone H2A and Cy5 on the exit end of the extranucleosomal DNA and anchored on a surface. Nucleosomes were positioned on DNA by a 601 nucleosome positioning sequence, leaving 3 bp of extranucleosomal DNA on the exit end and 78 bp of extranucleosomal DNA on the entry end (denoted as 78N3). A decrease in FRET value is expected to occur after the addition of ATP and ISW2, caused by nucleosomes moving towards the center of the DNA, thereby increasing the distance between the donor and acceptor dyes. The translocation distance of the nucleosomes was calculated by comparing the FRET values of the remodeled nucleosomes to a set of calibration nucleosomes with different exit linker DNA length. These calibration nucleosomes were made by keeping the Cy5 dye at the end of the exit extranucleosomal DNA and changing the extranucleosomal DNA length by repositioning the 601 nucleosome positioning sequence[26]. As expected, we observed ISW2 moving end-positioned nucleosomes (78N3) towards the center-positioned configuration with changes in FRET values from an initial value of ~0.87 to a near zero value (Fig. 7a). We note that a relatively high ATP concentration was used here to allow a fast remodeling rate. Hence the individual translocation steps were not resolved in the FRET time traces. Notably, ISW2 mostly translocated nucleosomes in a unidirectional manner and rarely reversed the direction of movement. Only 6% of the FRET traces showed direction reversal (Fig. 7b). mSLIDE however had a much greater tendency to change the direction of nucleosome movement. We found in approximately 54% of the FRET traces bidirectional nucleosome movement as reflected by both decrease and increase in FRET (Fig. 7c and 7b). By measuring the FRET values at the points of direction reversal, we found that most of the reversals (~70%) occurred after having moved ~7 bp; while a smaller number (~30%) moved only ~4 bp before changing direction (Fig. 7d). About 46% of the nucleosomes moved in one direction only and did not change direction during the observation time window before photobleaching occurred. In these cases, the nucleosomes appeared to be stalled after ~11 bp of movement (Fig. 7c, dwell times of at least ~47 s). Stable binding of SLIDE thus helps maintain the uni-directional movement of nucleosomes by ISW2.

Although binding of SLIDE domain is substantially weakened, it is evident that mSLIDE is still able to facilitate more typical remodeling at a reduced frequency as evident by nucleosomes being fully remodeled given sufficient time (Fig. 4a) and once the DNA exiting has moved at least 11 bp it is no longer able to back track (Fig. 7c).

Discussion

We found that the SLIDE domain of ISW2 has two roles: first, it binds the auxiliary subunit Itc1 as shown by deleting the SLIDE domain and second, it pushes linker DNA into nucleosomes as shown by mutating four basic residues in SLIDE. These residues when changed to alanine reduced primarily the interactions between the ISW2 complex and a part of extranucleosomal DNA spanning from 80 to 94 bp from the dyad axis as shown by DNA protection and site-directed DNA crosslinking (Fig. 2 and Fig. 3). These changes are consistent with prior crosslinking and peptide mapping experiments showing that the SLIDE domain binds extranucleosomal DNA 92 bp from the dyad axis[15]. SLIDE domain binding to extranucleosomal DNA is not required for proper docking of the ATPase domain to nucleosomal DNA at SHL2 or for the initial movement of the ATPase domain as shown by protection of DNA at the SHL2 site (compare Fig. 2a to 2b), site-directed crosslinking of Isw2 at nt-33 (Fig. 3d), and the initial changes in histone-DNA interactions near the dyad axis with the mSLIDE complex (Fig. 5).

The rates of nucleosome movement and ATP hydrolysis were respectively 1/9 and 1/7 that of WT when binding of the SLIDE domain to extranucleosomal DNA was diminished (Fig. 4b,d,e). The step most adversely affected in mSLIDE was extranucleosomal DNA movement into nucleosomes (Fig. 5) along with the formation of stable interactions with one DNA gyre of nucleosomes upon ATP hydrolysis that are associated with template commitment (Fig. 6). The SLIDE domain facilitates ISW2 moving DNA around the nucleosome in one preferred direction and avoids “back tracking” or direction reversals (Fig. 7). When the interactions of SLIDE are reduced ISW2 tends to shuttle DNA back and forth short distances at early stages in remodeling. This shuttling back and forth is rarely observed in wild type ISW2. It appears that SLIDE can have a regulatory like function in helping to maintain a single directional movement of DNA into nucleosomes. These data suggest a particular step is required in remodeling to establish the preferred direction of DNA movement that involves the SLIDE domain and could be connected to the SLIDE domain being required to push DNA into nucleosomes.

The molecular basis of ISW2 nucleosome spacing activity might be that linker DNA length regulates binding of the ATPase domain to SHL2 site and therefore assumes that the only engine to ATP-dependent nucleosome mobilization is the ATPase domain. While this is certainly one function of accessory subunits or additional domains, it is apparent for ISW2 that SLIDE domain contributions are more than just recruitment and indeed is part of the mechanical work needed for nucleosome movement. SLIDE bound to extranucleosomal DNA could push DNA into nucleosomes at the entry side through a conformation shift caused by ATP binding and/or hydrolysis (Fig. 8). Nucleosome spacing may therefore be regulated by two distinct mechanisms; one that lifts off the ATPase domain as linker DNA length is shortened and another that requires a sufficient length of linker DNA in order for ISW2 to push DNA into nucleosomes. The activities of the SLIDE and DNA translocase domains seem to be coordinated as evident by the ATPase and remodeling activities being comparably down regulated upon mutation of SLIDE. When the SLIDE domain is unable to bind and push DNA into nucleosomes, the ATPase domain is able to only move nucleosomal DNA ~10 bp before stalling.

ISWI remodelers have been known for several years to be distinct from SWI-SNF type remodelers in that they require a minimal length of extranucleosomal DNA for nucleosome remodeling. It now appears that this linker DNA requirement is not merely to provide a platform for binding of the remodeler, but rather reflects an intrinsic difference in the mechanism of chromatin remodeling between the ISWI and SWI-SNF family of chromatin remodelers. ISW2 needs to push DNA into nucleosomes and thus its grip on extranucleosomal DNA is important for remodeling and helps explain its requirement for linker DNA. SWI-SNF does not have this property and can remodel nucleosomes with no extranucleosomal DNA[27]. These features of ISW2 better explain how the ISWI class of remodelers can space nucleosomes.

Online Methods

Construction of Strains

Two copies of the FLAG epitope were attached to the C-terminus of *ISW2* by polymerase chain reaction (PCR). The wild type FLAG tagged *ISW2* gene was cloned to pET21d by cutting with Nco1 and Not1. A kanamycin (G418) cassette with 50 bp of sequence downstream of the endogenous *ISW2* gene was placed downstream of the fused Isw2-2FLAG by cutting with Not1. The resulting pISW2-Kan plasmid was linearized and transformed into BY 4742 and the appropriate gene replacement selected by kanamycin resistance. The SLIDE domain was deleted by two-step overlapping PCR[28] and transformed into strain BY4742. Mutations in the SLIDE domain were created by the Quick change method[29] using high fidelity Pfu ultra DNA polymerase (Stratagene) and confirmed by DNA sequencing.

Purification of ISW2 and ISW2 mutants

Wild type and mutant ISW2 was purified by immuno-affinity chromatography using M2 agarose (Sigma) and eluting with 1mg/ml FLAG peptide[30]. Protein purity was determined by analyzing samples on a 4–20% SDS–PAGE and stained with SyproRuby (Molecular Probes).

Nucleosome reconstitution

Mononucleosomes were assembled at 37°C with 8.5–10 μg of recombinant octamers, 100–200 fmol of ^{32}P labeled DNA, 10 μg of sonicated salmon sperm DNA or unlabeled DNA made by PCR and 1.8 M NaCl in a starting volume of 10 μl[31]. Samples were serially diluted as described to a final concentration of ~300 mM NaCl. Nucleosome assemblies were analyzed on a 4% native polyacrylamide gel (acrylamide:bisacrylamide; 35.36:1) in 0.5× TBE at 4°C. For smFRET experiments, a unique cysteine substitution was introduced at residue 120 of histone H2A, and a Cy3 donor dye (GE Healthcare) was attached to this cysteine residue. Cy3-labelled and unlabelled H2A were mixed at a ratio of 1:1 with other histone proteins (H2B, H3, and H4) to generate donor-labelled histone octamers. Dye-labelled mononucleosomes were reconstituted using these histone octamers and double-stranded DNA labelled with both a FRET acceptor dye (Cy5) and a biotin moiety at opposing ends. The 601 nucleosome positioning sequence was used to place the octamer on the DNA such that 3 bp of linker DNA remained on the exit side and 78 bp of linker DNA on the entry side.

Nucleosome Binding, Remodeling and ATPase Assays

ISW2 binding was at 30°C for 30 min in 35 mM HEPES-NaOH (pH 7.8), 5 mM $MgCl_2$, 80–100 mM NaCl, 0.1 mg/ml of bovine serum albumin, 5–8 % glycerol, and 40 μM 2-mercaptoethanol. Most remodeling assays contained 800 μM ATP. The rate of remodeling

was determined using saturating amounts of enzyme that was pre-bound to nucleosomes for 15 min at 30°C. Depending on the specific assay, remodeling was stopped either by the addition of only γ–S-ATP or the combination of salmon sperm DNA and γ–S-ATP. The extent of nucleosome-stimulated hydrolysis of ATP was measured pre-incubating nucleosomes and ISW2 for 30 min before addition of 7 μM γ-^{32}P ATP and further incubation for 10minutes. ATP and free phosphate were separated by thin layer chromatography on polyethyleneimine-cellulose.

Glycerol gradient centrifugation

Glycerol gradients (25–45%) were prepared in a solution of 5 mL with 100 mM Na HEPES pH 7.8, 10 mM Na EDTA pH 8.0, 0.2% NP-40 and 1M NaCl. On the top of the 5 mL solution layered 2 pico mole of ISW2 wild type or mSLIDE protein mixed with 25% glycerol containing the same buffer to make final volume 100μl. For the reaction with 50bp DNA, 3.75 μg 50 bp DNA from 601 sequence was used. The tubes were centrifuged for 20 hours at 4°C at 48500 rpm in a SW55 Ti rotor. Each 110μl fractions were collected from the bottom of the tube. 20μl of each fractions was analyzed by western blot (see below). Quantification of western blot signals was performed by Kodak 1D Imaging System. Molecular weight markers from Gel Filtration Molecular Weight Markers Kit for 29,000 – 700,000 Da (Sigma) contains carbonic anhydrase (29 kD), albumin (66 kD), yeast ADH (150 kD), β-amylase (200 kD), apoferritin (443 kD), thyroglobulin (669 kD) were separated in the same glycerol gradients followed by the same fraction collection. Fractions collected were analyzed by SDS-PAGE and SYPRO-Ruby (Molecular Probes) staining.

Western blot

All of the proteins are separated on SDS-PAGE and blotted onto Hybond-P PVDF membrane (GE Healthcare) using standard blotting techniques. The antibody used was anti-FLAG M2 peroxidase conjugate (1:1000 dilution, Sigma Catalog #A8592) SuperSignal West Femto Maximum Sensitivity Substrate (Thermo Scientific) was used for detection.

Hydroxyl radical footprinting

There are two different sets of cleavage conditions that were used to footprint the ISW2-nucleosome complexes. Both were performed as described previously[32] except that the final concentrations of Fe(II), H_2O_2, ascorbate and EDTA were different as well as the reaction times. The first set had 280 μM Fe(II), 0.17% H_2O_2, 5.7 mM ascorbate and 220 μM EDTA, and was incubated for 2 min. The second set was for more rapid footprinting of the remodeling reactions and contained 2 mM Fe(II), 0.15% H_2O_2, 5.7 mM ascorbate and 2.3 mM EDTA, and was reacted for only 30 s. The reactions were both terminated by addition of 100 μl of 5 M ammonium acetate, 5 mM thiourea and 10 mM EDTA. DNA was isolated by phenol: chloroform extraction, ethanol precipitation at −20° C and resolved in a denaturing 6.5% polyacrylamide gel with 8 M urea with a sequencing ladder of the same DNA. The gels were dried, phosphorimaged and data analyzed with ImageQuant and Microsoft Excel.

Site-specific DNA photoaffinity cross-linking

Site-specific photoreactive DNA probes were synthesized as described previously with phosphorothioate coupled to p-azido-phenacyl bromide using the 601 sequence[7, 33]. Oligonucleotides containing the phosphorothioate, 3 bp from the radiolabeled 5′ end were used for probe synthesis. Photoreactive DNA were reconstituted into end positioned nucleosomes (61-NPS-7) and bound with saturating amounts of ISW2 and mSLIDE for 30 min at 30°C. The extent of ISW2 binding was assessed on a 4% native gel. After binding ISW2 was crosslinked to DNA by UV irradiation (2 min at 310 nm, 2.65mW/cm2), and then

digested with DNase I and S1 nuclease. The crosslinked proteins were separated by 4–20% SDS–PAGE and visualized by phosphorimaging.

Single-molecule FRET

Dye labelled mononucleosomes were surface-anchored on PEG-coated quartz slides through biotin-streptavidin linkage and excited with a 532 nm laser, and fluorescence emission from Cy3 and Cy5 was detected as described previously[26]. Wild-type or mutant ISW2 complex was added to the surface-anchored nucleosomes together with ATP to induce remodelling. The presence of two H2A subunits in each histone octamer gives rise to a heterogeneous population of nucleosomes with three different labelling configurations that can be unambiguously separated in FRET measurements at the single molecule level. In this work, we selected nucleosomes containing a single donor on the proximal H2A as previously described[26] and restricted our analyses to this homogenous population. The imaging buffer contained 12 mM HEPES, 40 mM Tris pH 7.5, 60 mM KCl, 0.32 mM EDTA, 3 mM $MgCl_2$, 10 % glycerol, 0.02% Igepal (Sigma Aldrich), an oxygen scavenging system (10 % glucose, 800 μg ml^{-1} glucose oxidase, 40 μg ml^{-1} catalase), 2 mM Trolox (Sigma), and 0.1 mg ml^{-1} BSA (Promega). For the quantification of direction reversals in wild-type and mutant ISW2 traces, at least 100 FRET traces that displayed remodelling activity were first smoothed with a 20-pt mean filter to remove FRET fluctuations due to noise and direction reversals with FRET changes >0.1 were identified.

Site-directed histone DNA crosslinking

Site directed histone-DNA crosslinking were performed as described previously[19]. Briefly, histone octamer containing cysteine at residue 45 of H2A was reconstituted into mononucleosomes and conjugated to para-azido phenacyl bromide (APB). APB modified nucleosomes were mobilized with either ISW2 or mSLIDE for certain periods of time and stopped by adding excess ATPγS (4mM) and immediately UV crosslinked at 312 nm for 3 min. Samples were denatured by adding SDS to 1% and heating at 70°C for 20 min. The histone-DNA conjugates were purified by phenol-chlorofom extraction and ethanol precipitation. DNA was resuspended in alkaline cleavage buffer of 2% SDS, 20 mM ammonium acetate, 0.1 mM EDTA and cleaved by incubation with 0.1M NaOH for 45 min at 90°C. The cleaved DNA was neutralized using HCl, purified by ethanol precipitation and resuspended in 95% formamide + dye. Cleaved DNA was resolved in a 6.5 % denaturing polyacrylamide gel along with a sequence ladder of the same DNA. The bands were visualized by phosphorimaging and analyzed further by ImageQuant. Normalized lane intensities were plotted and overlaid using Microsoft Excel.

Supplementary Material

Refer to Web version on PubMed Central for supplementary material.

Acknowledgments

We would like to thank Nilanjana Chatterjee for construction of the yeast strain for Isw2 catalytic subunit purification, and members of the Bartholomew laboratory for their input. This work was funded by National Institutes of Health GM 48413 (BB) and the Howard Hughes Medical Institute (X.Z.). S.D. is a Merck Fellow of the Jane Coffin Childs Memorial Fund for Medical Research.

References

1. Becker PB, Horz W. ATP-dependent nucleosome remodeling. Annu Rev Biochem. 2002; 71:247–273. [PubMed: 12045097]

2. Gangaraju VK, Bartholomew B. Mechanisms of ATP dependent chromatin remodeling. Mutat Res. 2007; 618:3–17. [PubMed: 17306844]
3. Clapier CR, Cairns BR. The biology of chromatin remodeling complexes. Annu Rev Biochem. 2009; 78:273–304. [PubMed: 19355820]
4. Hota SK, Bartholomew B. Diversity of operation in ATP-dependent chromatin remodelers. Biochim Biophys Acta. 2011
5. Zofall M, Persinger J, Bartholomew B. Functional role of extranucleosomal DNA and the entry site of the nucleosome in chromatin remodeling by ISW2. Mol Cell Biol. 2004; 24:10047–10057. [PubMed: 15509805]
6. Yang JG, Madrid TS, Sevastopoulos E, Narlikar GJ. The chromatin-remodeling enzyme ACF is an ATP-dependent DNA length sensor that regulates nucleosome spacing. Nat Struct Mol Biol. 2006; 13:1078–1083. [PubMed: 17099699]
7. Kagalwala MN, Glaus BJ, Dang W, Zofall M, Bartholomew B. Topography of the ISW2-nucleosome complex: insights into nucleosome spacing and chromatin remodeling. Embo J. 2004; 23:2092–2104. [PubMed: 15131696]
8. Stockdale C, Flaus A, Ferreira H, Owen-Hughes T. Analysis of nucleosome repositioning by yeast ISWI and Chd1 chromatin remodeling complexes. J Biol Chem. 2006; 281:16279–16288. [PubMed: 16606615]
9. Dang W, Kagalwala MN, Bartholomew B. Regulation of ISW2 by concerted action of histone H4 tail and extranucleosomal DNA. Mol Cell Biol. 2006; 26:7388–7396. [PubMed: 17015471]
10. Gangaraju VK, Prasad P, Srour A, Kagalwala MN, Bartholomew B. Conformational changes associated with template commitment in ATP-dependent chromatin remodeling by ISW2. Mol Cell. 2009; 35:58–69. [PubMed: 19595716]
11. Dang W, Kagalwala MN, Bartholomew B. The Dpb4 subunit of ISW2 is anchored to extranucleosomal DNA. J Biol Chem. 2007; 282:19418–19425. [PubMed: 17491017]
12. Dang W, Bartholomew B. Domain architecture of the catalytic subunit in the ISW2-nucleosome complex. Mol Cell Biol. 2007; 27:8306–8317. [PubMed: 17908792]
13. Aasland R, Stewart AF, Gibson T. The SANT domain: a putative DNA-binding domain in the SWI-SNF and ADA complexes, the transcriptional co-repressor N-CoR and TFIIIB. Trends Biochem Sci. 1996; 21:87–88. [PubMed: 8882580]
14. Grune T, et al. Crystal structure and functional analysis of a nucleosome recognition module of the remodeling factor ISWI. Mol Cell. 2003; 12:449–460. [PubMed: 14536084]
15. Yamada K, et al. Structure and mechanism of the chromatin remodelling factor ISW1a. Nature. 2011; 472:448–453. [PubMed: 21525927]
16. Pinskaya M, Nair A, Clynes D, Morillon A, Mellor J. Nucleosome remodeling and transcriptional repression are distinct functions of Isw1 in Saccharomyces cerevisiae. Mol Cell Biol. 2009; 29:2419–2430. [PubMed: 19273607]
17. Eberharter A, Vetter I, Ferreira R, Becker PB. ACF1 improves the effectiveness of nucleosome mobilization by ISWI through PHD-histone contacts. Embo J. 2004; 23:4029–4039. [PubMed: 15457208]
18. Dechassa ML, et al. Disparity in the DNA translocase domains of SWI/SNF and ISW2. Nucleic Acids Res. 2012; 40:4412–4421. [PubMed: 22298509]
19. Kassabov SR, Bartholomew B. Site-directed histone-DNA contact mapping for analysis of nucleosome dynamics. Methods Enzymol. 2004; 375:193–210. [PubMed: 14870668]
20. Kassabov SR, Henry NM, Zofall M, Tsukiyama T, Bartholomew B. High-resolution mapping of changes in histone-DNA contacts of nucleosomes remodeled by ISW2. Mol Cell Biol. 2002; 22:7524–7534. [PubMed: 12370299]
21. Ong MS, Richmond TJ, Davey CA. DNA stretching and extreme kinking in the nucleosome core. J Mol Biol. 2007; 368:1067–1074. [PubMed: 17379244]
22. Richmond TJ, Davey CA. The structure of DNA in the nucleosome core. Nature. 2003; 423:145–150. [PubMed: 12736678]
23. Luger K, Mader AW, Richmond RK, Sargent DF, Richmond TJ. Crystal structure of the nucleosome core particle at 2.8 A resolution. Nature. 1997; 389:251–260. [PubMed: 9305837]

24. Hall MA, et al. High-resolution dynamic mapping of histone-DNA interactions in a nucleosome. Nat Struct Mol Biol. 2009; 16:124–129. [PubMed: 19136959]
25. Brower-Toland BD, et al. Mechanical disruption of individual nucleosomes reveals a reversible multistage release of DNA. Proc Natl Acad Sci U S A. 2002; 99:1960–1965. [PubMed: 11854495]
26. Blosser TR, Yang JG, Stone MD, Narlikar GJ, Zhuang X. Dynamics of nucleosome remodelling by individual ACF complexes. Nature. 2009; 462:1022–1027. [PubMed: 20033040]
27. Dechassa ML, et al. SWI/SNF has intrinsic nucleosome disassembly activity that is dependent on adjacent nucleosomes. Mol Cell. 2010; 38:590–602. [PubMed: 20513433]
28. Shevchuk NA, et al. Construction of long DNA molecules using long PCR-based fusion of several fragments simultaneously. Nucleic Acids Res. 2004; 32:e19. [PubMed: 14739232]
29. McClelland M, Nelson M. Effect of site-specific methylation on DNA modification methyltransferases and restriction endonucleases. Nucleic Acids Res. 1992; 20(Suppl):2145–2157. [PubMed: 1317957]
30. Tsukiyama T, Palmer J, Landel CC, Shiloach J, Wu C. Characterization of the imitation switch subfamily of ATP-dependent chromatin-remodeling factors in Saccharomyces cerevisiae. Genes Dev. 1999; 13:686–697. [PubMed: 10090725]
31. Lorch Y, LaPointe JW, Kornberg RD. Nucleosomes inhibit the initiation of transcription but allow chain elongation with the displacement of histones. Cell. 1987; 49:203–210. [PubMed: 3568125]
32. Tullius TD, Dombroski BA, Churchill ME, Kam L. Hydroxyl radical footprinting: a high-resolution method for mapping protein-DNA contacts. Methods Enzymol. 1987; 155:537–558. [PubMed: 2828876]
33. Sengupta SM, et al. The interactions of yeast SWI/SNF and RSC with the nucleosome before and after chromatin remodeling. J Biol Chem. 2001; 276:12636–12644. [PubMed: 11304548]

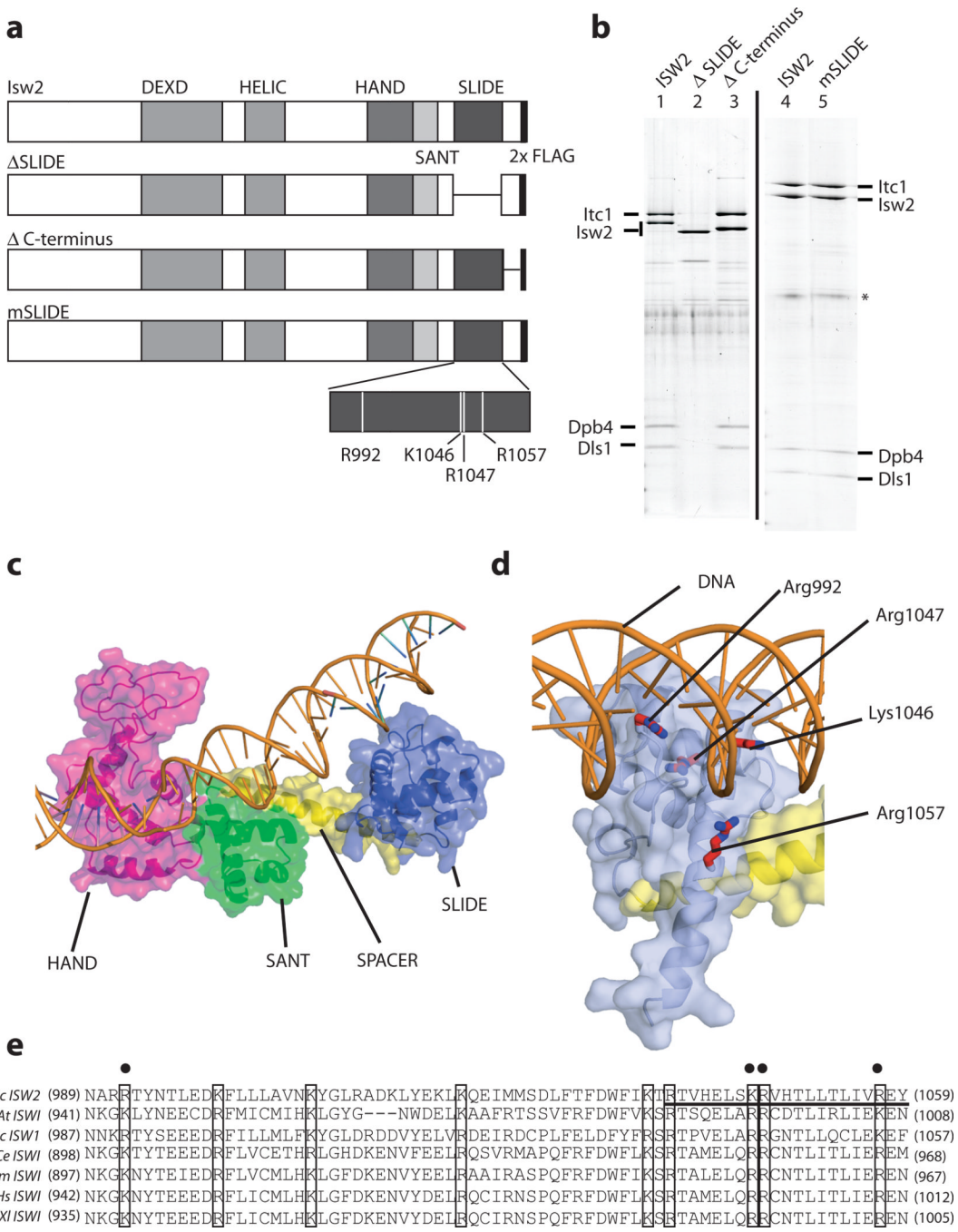

Figure 1.

SLIDE domain is required for ISW2 complex assembly. (**a**) The locations of the conserved motifs/domains in the ATPase domain (DEXD and HELIC) and C-terminus of Isw2 are shown. Two regions of Isw2 were separately deleted, ΔSLIDE (residues 974–1083) and Δ C-terminus (residues 1054–1120). In a third construct (mSLIDE) four conserved basic residues were changed to alanine. All constructs contained two copies of the FLAG epitope at the C-terminus for purification. (**b**) We determined the complex integrity of all three mutant ISW2 complexes by immunopurification and SDS-PAGE (4–20%). Bovine serum albumin was present in all of the purified enzymes and is marked by an *****. (**c**) The model of

the structure of the C-terminus of Isw2 based on sequence homology with the Drosophila ISWI C-terminus is shown with the HAND, SANT, spacer, and SLIDE domains highlighted. (**d**) The four conserved residues in SLIDE changed to alanine are labeled in the Isw2 model. (**e**) have been aligned and The conserved basic residues of SLIDE domains from various ISWI proteins are shown with the residues boxed. The black dots indicated the amino acid residues that are likely to bind extranucleosomal DNA and the region crosslinked to extranucleosomal DNA underlined.

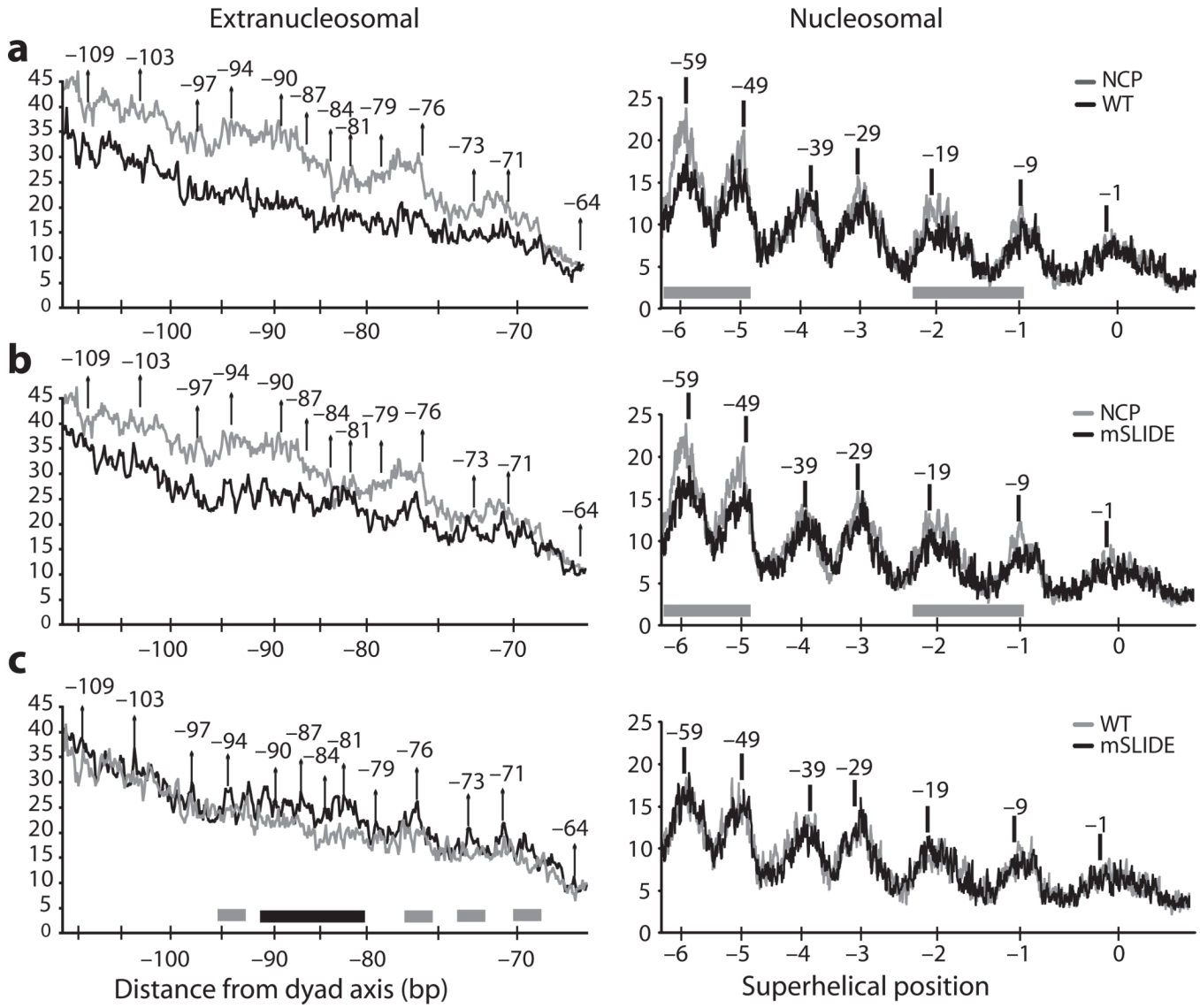

Figure 2.

Stable binding of the SLIDE domain to extranucleosomal DNA requires four conserved basic residues in SLIDE. (**a**) Interactions of ISW2 with nucleosomes were changed at specific location in extranucleosomal DNA when the SLIDE domain was mutated. The extent of DNA protected with nucleosome alone (grey) and with nucleosome bound by ISW2 (black) are shown for the extranucleosomal (left panel) and nucleosomal DNA regions (right panel). The x-axis for nucleosomal DNA refers to the SHL or super helical position (−6 to 0) and for extranucleosomal DNA the numbering refers to the number of bp from the dyad axis. The regions protected by ISW2 in the nucleosomal DNA region are highlighted by grey horizontal bars. (**b**) The analysis for mSLIDE-nucleosome complexes are the same as for WT-ISW2 in (**a**). (**c**) The two footprint patterns for WT-nucleosomes (grey) and mSLIDE-nucleosomes (black) are overlaid for comparison. The regions that were protected less by mSLIDE than those protected by WT are highlighted by horizontal grey and black bars in the extranucleosomal region (left side).

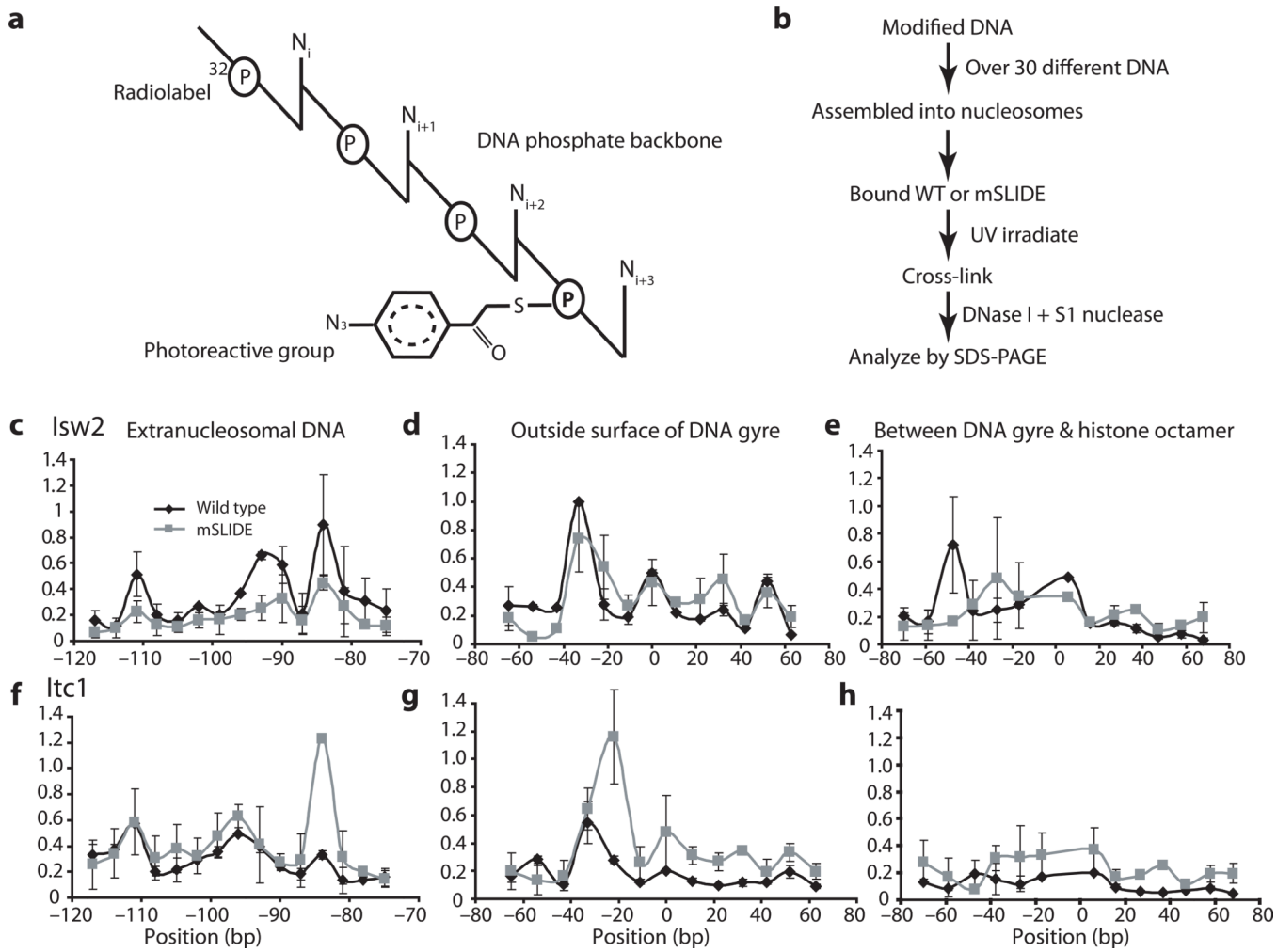

Figure 3.

Binding of mSLIDE to nucleosomes is altered from wild type ISW2 (WT). (**a**) The interactions of ISW2 with nucleosomes were investigated by site-specific DNA crosslinking using an aryl azide tethered to the phosphate backbone of DNA as shown. A ^{32}P radiolabel was incorporated 3 nucleotides from the photoreactive site. (**b**) Twenty eight different photoreactive DNA were each separately incorporated into nucleosomes. The modified nucleosomes after binding WT or mSLIDE were crosslinked by UV irradiation and processed as described before loading on to an SDS-PAGE. (**c–h**) The crosslinking intensities for Isw2 (**c–e**) and Itc1 (**f–h**) are shown relative to crosslinked Isw2 at nt −33 as a range from two experiments. The relative crosslinking efficiencies are plotted for extranucleosomal DNA (**c & f**); and the exposed (**d & g**) and protected (**e & h**) surfaces of the DNA gyre.

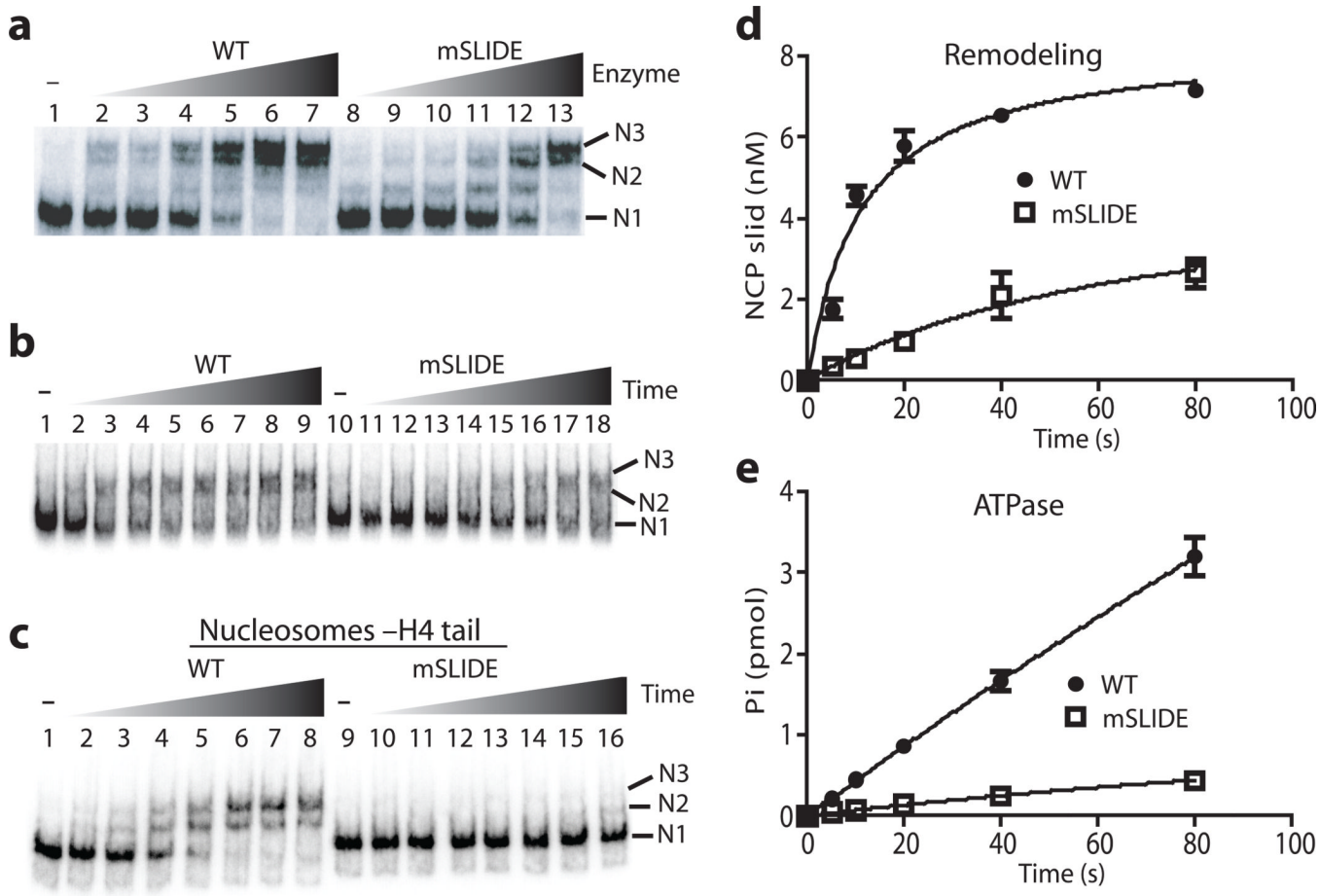

Figure 4.

SLIDE domain is required for nucleosome movement and ATP hydrolysis. (**a**) The efficiency of nucleosome mobilization by mSLIDE was compared to WT by titrating the amount of enzyme (0.125 to 4 nM) with a fixed amount of nucleosomes (16 nM) and ATP (800 μM) followed by analysis on a 5% native polyacrylamide gel. Lane 1 had no ISW2 added. N1 refers to the position of unremodeled nucleosomes and N2 and N3 to the positions of remodeled nucleosomes. (**b**) Remodeling by WT (lanes 2–9) and mSLIDE (lanes 11–18) was compared by measuring the rate at which each moves nucleosomes (16 nM) with saturating amounts of enzyme (96 nM). Enzymes were competed off before analyzing by gel shift. Lanes 1 and 10 had no enzyme added. (**c**) The rate of nucleosome movement was measured the same as in (**b**), except that the nucleosomes used were missing the histone H4 tail (residues 1– 27). The reactions contained WT (lanes 2–8) or mSLIDE (lanes 10–16). (**d**) The amount of nucleosomes moved from their original position was plotted versus reaction time. The rate of nucleosome movement for WT (closed circle) and mSLIDE (open square) was 0.62 ± 0.06 and 0.066 ± 0.015 nM nucleosomes per second (s.d., n=4). (**e**) The amount of inorganic phosphate generated under the same conditions as in (b) was plotted versus time. The rate of ATP hydrolysis was 5.7±2.5 and 40±8.0 fmoles ADP per second for mSLIDE and ISW2 (s.d., n=3).

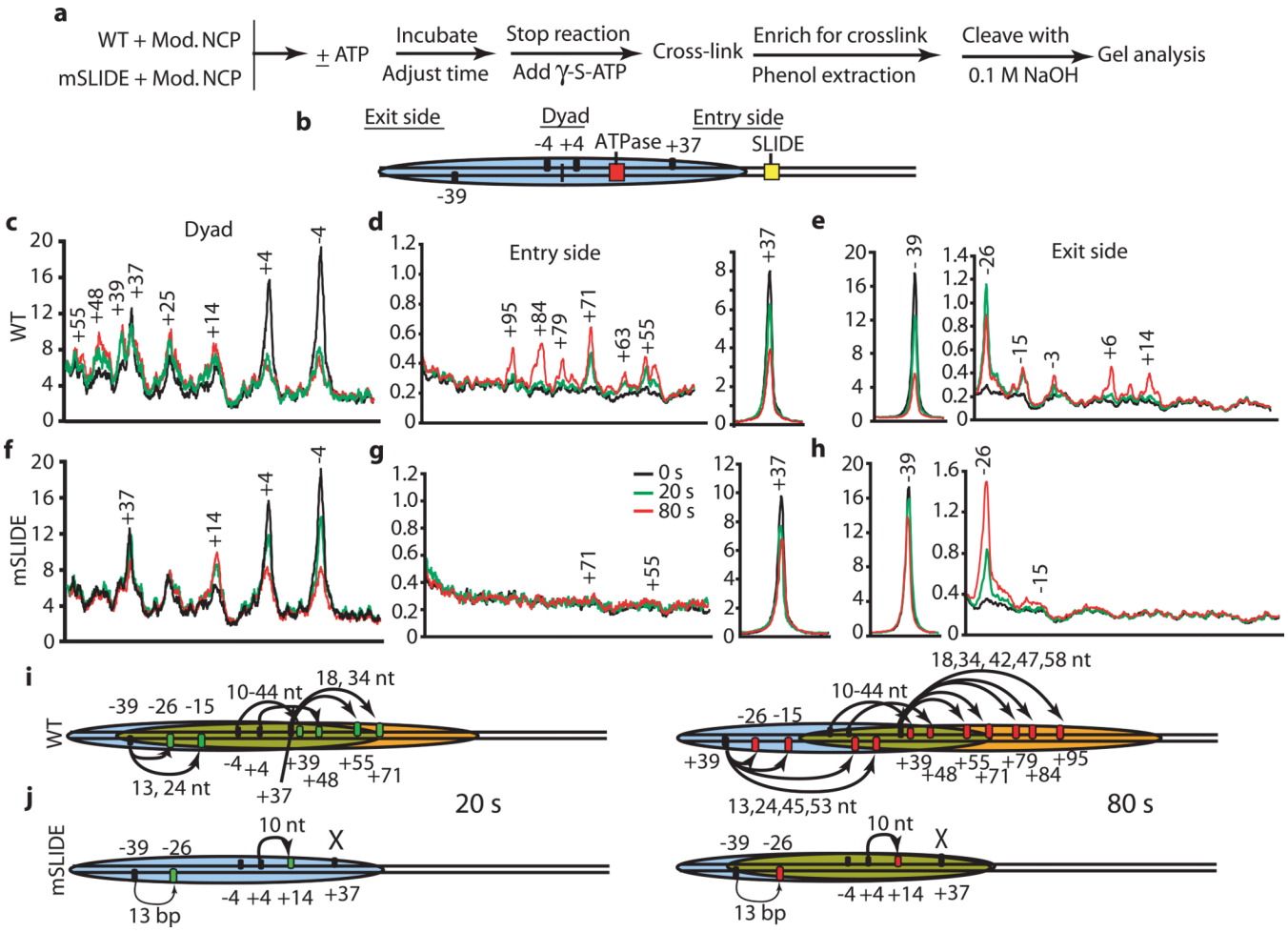

Figure 5.

The SLIDE domain helps move DNA into nucleosomes. (**a**) The order of additions and different steps in remodeling, crosslinking, and detecting the DNA crosslinking site are shown. Nucleosome remodeling was stopped by the addition of 4 mM γ-S-ATP thereby keeping ISW2 bound and poised before irradiating and processing as described[19]. The particular histone site monitored was determined by varying the modification site and the DNA strand that was radiolabeled. (**b**) The arrangements of cut sites and their strand specificity are shown along with the locations where the DNA translocase and SLIDE domains are bound. (**c–h**) Changes in histone-DNA contact close to the dyad axis (**c,f**) and where DNA enters into nucleosome (entry side, **d, g**), and DNA exits from the nucleosome (exit side, **e, g**) are shown for WT (**c–e**) and mSLIDE (**f–h**). The relative intensity of DNA cleavage is shown for the starting position (black), and for 20 (green) and 80 s (red) after addition of enzyme and ATP. (**i–j**) The movements of DNA relative to the histone octamer versus the original positions (black) are depicted at 20 (green) and 80 (red) s after addition of ATP for WT (**i**) and mSLIDE (**j**). The regions occupied by nucleosomes prior to remodeling (blue) and during remodeled (orange) are shown.

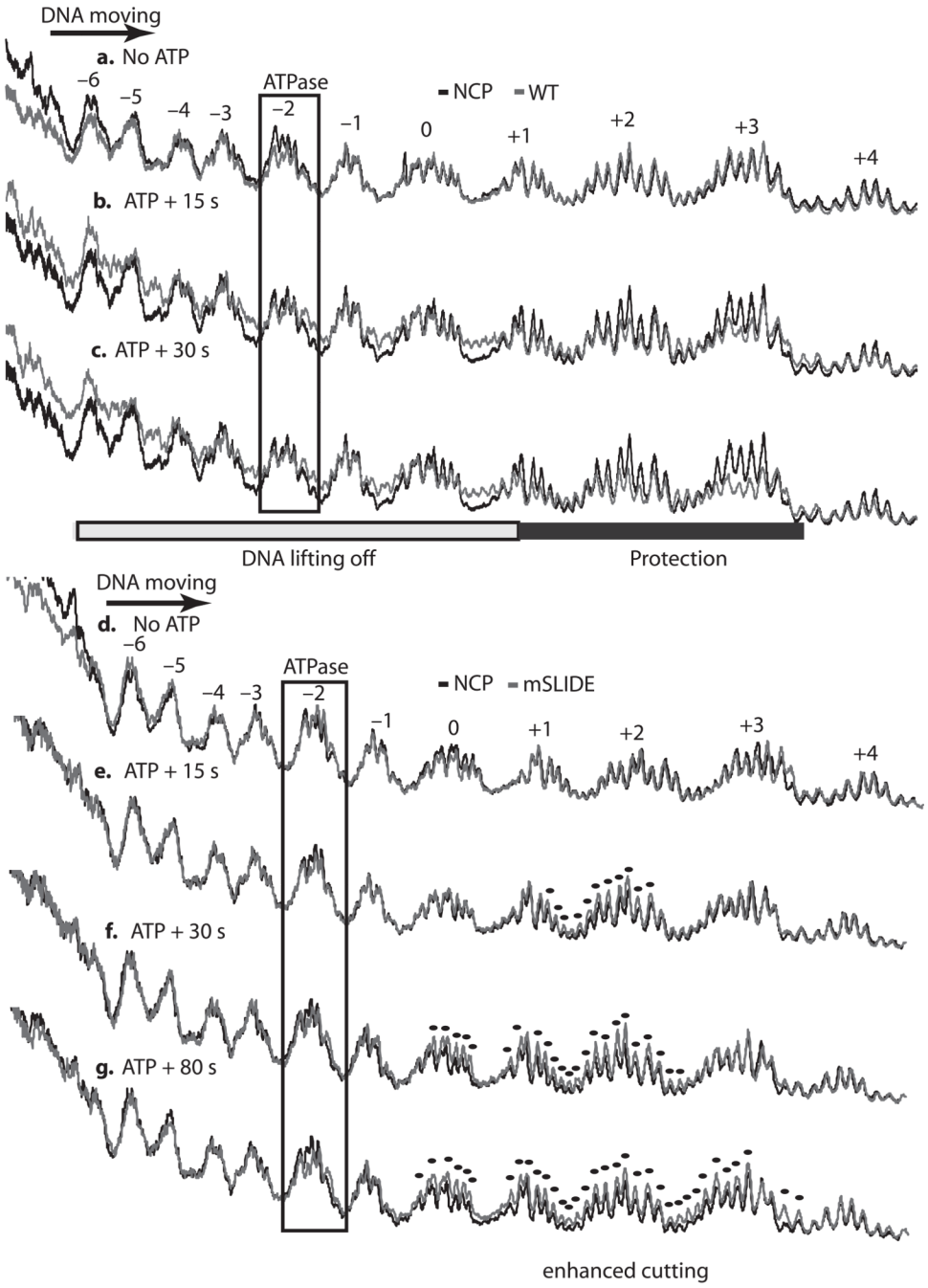

Figure 6.

Certain regions in nucleosomal DNA are preferentially altered during remodeling by mSLIDE. Changes in nucleosomal structure that occur during WT and mSLIDE remodeling were probed by protection to hydroxyl radial cleavage. Nucleosomes (0N70) were fully bound to WT (a–c) or mSLIDE (d–g) at 30°C for 15 min. Reactions were cooled to 25°C before ATP was added. Remodeling was for 15 (b,e), 30 (c,f), or 80 (g) s before the complexes were exposed to hydroxyl radical for 30 s. The numbering refers to the superhelical position of the DNA and the black dots highlight those positions where enhanced cleavage due to mSLIDE remodeling occurred. The direction which DNA is moving relative to nucleosomes during remodeling is also shown.

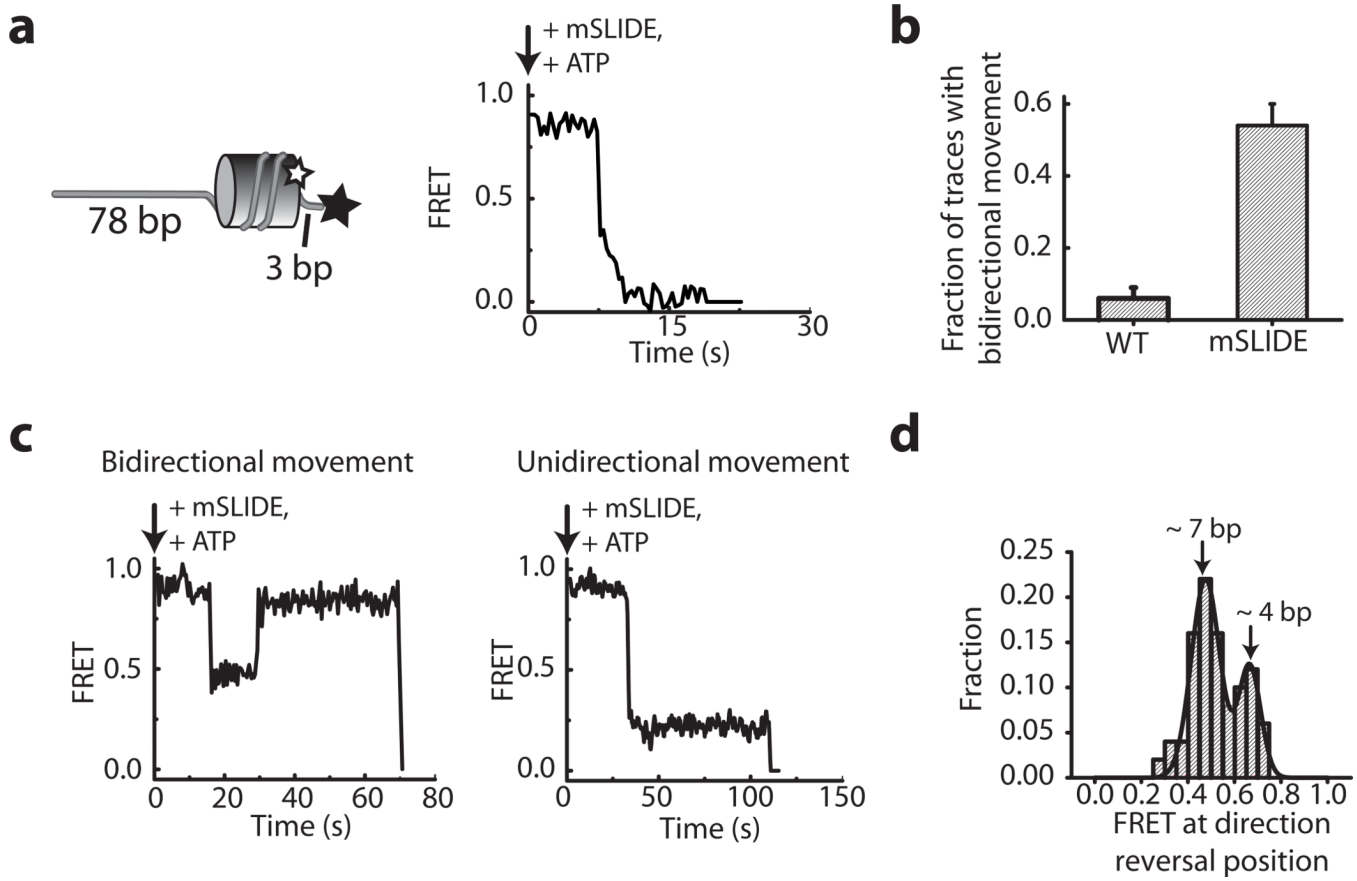

Figure 7.

Stable binding of the SLIDE domain promotes the uni-directional movement of DNA exiting nucleosomes in ISW2 remodeling. (**a**) Single-molecule (sm) FRET was used to measure the dynamics of DNA exiting nucleosomes during remodeling. Nucleosomes (78N3) had the donor dye Cy3 attached to cysteine incorporated at residues 120 of H2A (open star) and an acceptor dye Cy5 to the DNA 3 bp from the edge of the nucleosome (closed star). A typical FRET trace of nucleosome remodeling by ISW2 with 1.5 mM ATP is shown. (**b**) The fractions of traces with ISW2 (6%) and mSLIDE (54%) with direction reversals are shown (s.d., n>100). (**c**) FRET traces of nucleosome remodeling by mSLIDE. The left trace is typical of those showing direction reversals and the right trace for those showing unidirectional translocation. At the relatively high ATP concentration of 1.5 mM, the remodeling rate is fast and individual translocation steps are not resolved here. (**d**) This histogram shows the lowest FRET plateau just before the first direction reversal occurs. About 70 % of all reversal plateaus occur at a FRET value of 0.47 (left peak) and correspond to a translocation of ~6.8 bp from the initial nucleosome position. The remaining 30% reversal plateaus occur at a mean FRET of 0.66 (right peak), corresponding to a translocation of ~3.6 bp away from the starting position.

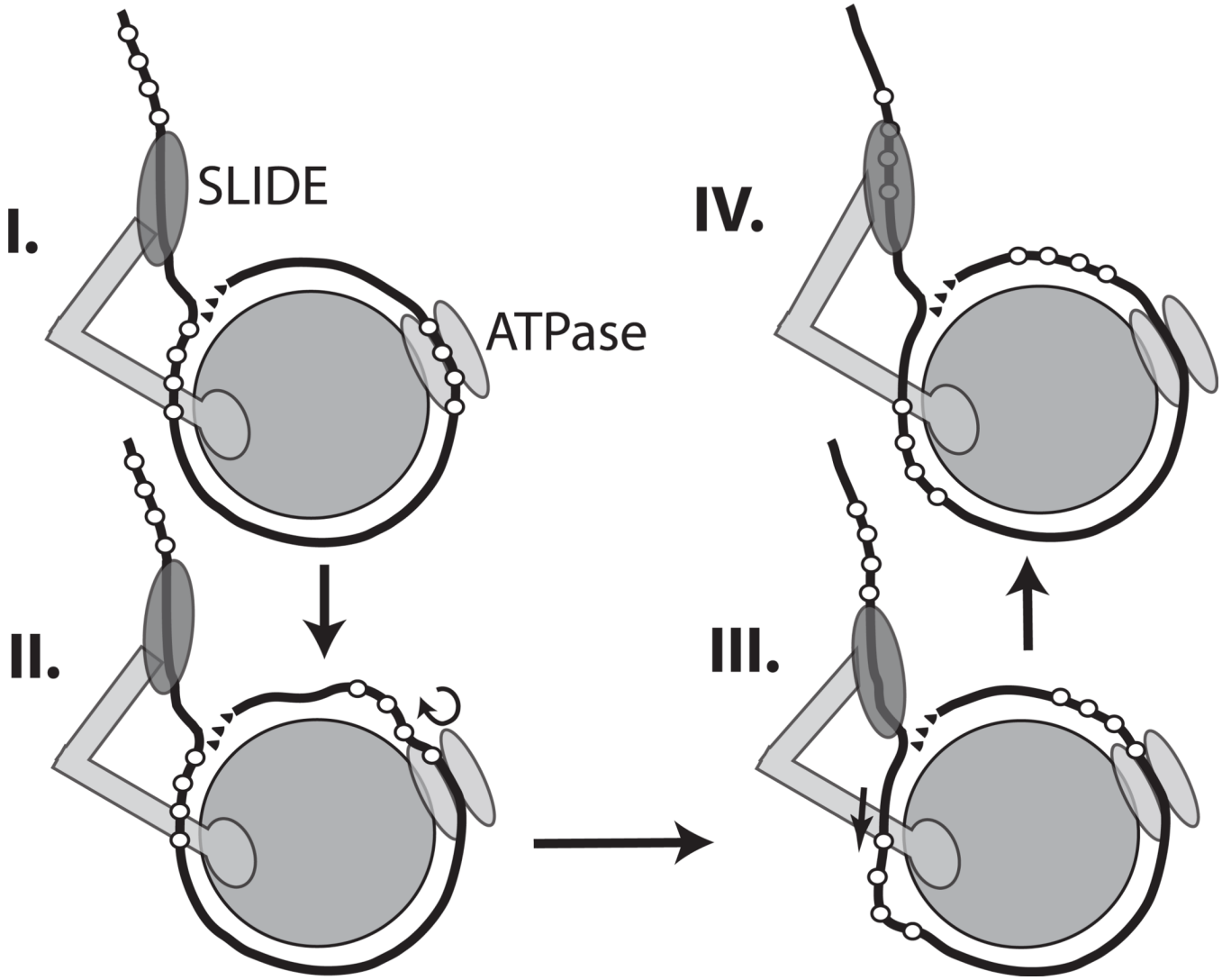

Figure 8.

The actions of the DNA translocase and SLIDE domains are both required for moving nucleosomes as shown in this model. (I) The SLIDE domain bound to extranucleosomal DNA is tethered to the histone octamer. (II) The initial step in remodeling is the translocation of the ATPase domain at the SHL2 site. (III) The conformation of the tether is changed thereby bringing the SLIDE domain closer to the histone anchor and pushes DNA into the nucleosome. (IV) The ATPase domain moves DNA pushed in by the SLIDE domain further inside of nucleosomes. The SLIDE domain will need to release its hold on DNA and rebind at a new DNA site in order to reset itself for additional movement of DNA into the nucleosome.